Received: 13 July 2019 | Revised: 19 October 2019 | Accepted: 6 November 2019

DOI: 10.1096/fj.201901686R

RESEARCH ARTICLE

THE FASEB JOURNAL

In vivo real-time ATP imaging in zebrafish hearts reveals G0s2 induces ischemic tolerance

Hidetaka Kioka[1] | Hisakazu Kato[2] | Takeshi Fujita[1,3] | Yoshihiro Asano[1] | Yasunori Shintani[4] | Satoru Yamazaki[4] | Osamu Tsukamoto[2] | Hiromi Imamura[5] | Mikihiko Kogo[3] | Masafumi Kitakaze[6] | Yasushi Sakata[1] | Seiji Takashima[2,7]

[1]Department of Cardiovascular Medicine, Osaka University Graduate School of Medicine, Suita, Japan

[2]Department of Medical Biochemistry, Osaka University Graduate School of Medicine, Frontier Bioscience, Suita, Japan

[3]First Department of Oral and Maxillofacial Surgery, Graduate School of Dentistry, Osaka University, Suita, Japan

[4]Department of Molecular Pharmacology, National Cerebral and Cardiovascular Center Research Institute, Suita, Japan

[5]Graduate School of Biostudies, Kyoto University, Kyoto, Japan

[6]Department of Clinical Research and Development, National Cerebral and Cardiovascular Center Research Institute, Suita, Japan

[7]Japan Science and Technology Agency-Core Research for Evolutional Science and Technology (CREST), Kawaguchi, Japan

Correspondence
Hidetaka Kioka and Yoshihiro Asano, Department of Cardiovascular Medicine, Osaka University Graduate School of Medicine, Suita, Osaka 565-0871, Japan.
Email: kioka@cardiology.med.osaka-u.ac.jp (H. K.) and asano@cardiology.med.osaka-u.ac.jp (Y. A.)

Funding information
Japan Agency for Medical Research and Development (AMED), Grant/Award Number: 19ek0109412h0001; MEXT | JST | Core Research for Evolutional Science and Technology (CREST), Grant/Award Number: JPMJCR14M2

Abstract

Most eukaryotic cells generate adenosine triphosphate (ATP) through the oxidative phosphorylation system (OXPHOS) to support cellular activities. In cultured cell-based experiments, we recently identified the hypoxia-inducible protein G0/G1 switch gene 2 (G0s2) as a positive regulator of OXPHOS, and showed that G0s2 protects cultured cardiomyocytes from hypoxia. In this study, we examined the in vivo protective role of G0s2 against hypoxia by generating both loss-of-function and gain-of-function models of *g0s2* in zebrafish. Zebrafish harboring transcription activator-like effector nuclease (TALEN)-mediated knockout of *g0s2* lost hypoxic tolerance. Conversely, cardiomyocyte-specific transgenic zebrafish hearts exhibited strong tolerance against hypoxia. To clarify the mechanism by which G0s2 protects cardiac function under hypoxia, we introduced a mitochondrially targeted FRET-based ATP biosensor into zebrafish heart to visualize ATP dynamics in in vivo beating hearts. In addition, we employed a mosaic overexpression model of *g0s2* to compare the contraction and ATP dynamics between *g0s2*-expressing and non-expressing cardiomyocytes, side-by-side within the same heart. These techniques revealed that *g0s2*-expressing cardiomyocyte populations exhibited preserved contractility coupled with maintained intra-mitochondrial ATP concentrations even under hypoxic condition. Collectively, these results demonstrate that G0s2 provides ischemic tolerance in vivo by maintaining ATP production, and therefore represents a promising therapeutic target for hypoxia-related diseases.

Abbreviations: ATeam, ATP indicator based on Epsilon subunit for Analytical Measurement; ATGL, adipose triglyceride lipase; ATP, adenosine triphosphate; $[ATP]_{mito}$, intra-mitochondrial ATP concentration; CO, cardiac output; dpf, days post-fertilization; FCCP, 2-[2-[4-(trifluoromethoxy)phenyl] hydrazinylidene]-propanedinitrile; FRET, Förster resonance energy transfer; G0s2, G0/G1 switch gene 2; HD, hydrophobic domain; KO, knockout; NRVCs, neonatal rat ventricular cardiomyocytes; OXPHOS, oxidative phosphorylation system; PMF, proton motive force; RFLP, restriction fragment length polymorphism; TALEN, transcription activator-like effector nucleases.

KEYWORDS
ATP, energy metabolism, FRET, in vivo imaging, ischemic tolerance

1 | INTRODUCTION

Mitochondria generate most cellular adenosine triphosphate (ATP) by substrate oxidation, mainly via the oxidative phosphorylation (OXPHOS) system. Oxygen plays a fundamental role in the production of ATP through OXPHOS. Mitochondrial ATP production must be maintained at a level that meets the cells' needs, even under stressful conditions such as hypoxia. Indeed, hypoxic stimuli increase OXPHOS efficiency to increase ATP production under hypoxia.[1-3] These adaptive mechanisms for maintaining energy homeostasis are especially important in metabolically active organs such as the heart.[4,5] However, the precise molecular mechanism for maintaining energy homeostasis remains unknown, particularly in vivo.

We have recently established a method for the selective evaluation of intra-mitochondrial ATP levels in primary cultured neonatal rat ventricular cardiomyocytes (NRVCs) using a mitochondrially targeted FRET-based ATP biosensor named Mit-ATeam.[6-8] Using this method, we identified the hypoxia-inducible protein G0/G1 switch gene (G0s2) as an activator of ATP production.[7] Biochemical analyses and cell biological experiments demonstrated that G0s2 interacts with F_oF_1-ATP synthase, also known as mitochondrial respiratory complex V, via its hydrophobic domain (HD), thereby increasing mitochondrial ATP production. Furthermore, we showed that G0s2 protects NRVCs from hypoxia-induced cell death by maintaining ATP production. However, because the energy metabolism in cultured cells may be different from that in the living tissues,[9,10] the in vivo protective effect of G0s2 against hypoxia must be evaluated.

In this study, we investigated the in vivo protective role of G0s2 under hypoxia using TALEN-mediated *g0s2* knockout (KO) and cardiomyocyte-specific *g0s2* transgenic zebrafish. Furthermore, to clarify the mechanism by which overexpressed G0s2 protects cardiac function, we also established an in vivo ATP imaging technique by introducing Mit-ATeam into zebrafish hearts. Our findings suggest that G0s2 protects tissue function by maintaining ATP production under limited oxygen condition.

2 | MATERIALS AND METHODS

2.1 | RNA extraction from zebrafish and quantitative RT-PCR

Eight to ten larvae at 5 days post-fertilization (dpf) were homogenized with RNA-Bee reagent (Tel-Test, Friendswood, TX, USA) and converted to cDNA using Omniscript RT kit (Qiagen, Venlo, Netherlands) according to the manufacturer's instructions. Quantitative RT-PCR was performed with SYBR Green technology and StepOnePlus Real-Time PCR Systems (Applied Biosystems, Foster City, CA, USA). Primer sequences were as follows:

g0s2 Fw 1, ACCACCGACAAACAAGGAATTATCATCCGA

g0s2 Rv 1, CTTGGCGAAAGGGATGAGCTCATGCATGGT

g0s2 Fw 2, GCGCTGGTCCCTCAAAAGGCTCTCTGAAGA

g0s2 Rv 2, GAGGGAAGATGCCACCTGGACCACTCCGCT

actb Fw, GGACTTCGAGCAGGAGATGGGAACCGCT

actb Rv, CATTGCCGATGGTGATGACCTGACCGTCA

The primer set with *g0s2* Fw 1+*g0s2* Rv 1 was used to amplify endogenous *g0s2* alone in Figure 1A. The primer set with *g0s2* Fw 2+*g0s2* Rv 2 was used to amplify overexpressed *g0s2* as well as endogenous *g0s2* in Figures 2B and 6B. *g0s2* mRNA expression levels were normalized to *actb* mRNA, used as an internal control gene, and the normalized values are presented as "relative *g0s2* mRNA level."

2.2 | Isolation and culture of zebrafish cardiomyocyte

In vitro culture of adult zebrafish cardiomyocytes is based on the method of NRVCs with some modifications.[11] Briefly, 20-25 of 3-month-adult Mit-ATeam fishes were anesthetized with 0.5 mg/mL of tricaine. Hearts were isolated from adult zebrafish under stereoscopic microscope and digested with 0.5 mg/mL of collagenase type II (Worthington, Columbus, OH, USA). After centrifugation, cell pellets were suspended with Leibovitz's L-15 media (Invitrogen, Carlsbad, CA, USA) containing 15% heat-inactivated fish serum (Meridian Life Science, Memphis, TN, USA). Cells were then plated onto collagen-coated 35-mm glass dish (Iwaki, Shizuoka, Japan).

2.3 | *g0s2* TALEN mutagenesis

2.3.1 | Construction of TALEN plasmids

The *g0s2* TALEN target site was selected using the online TAL Effector-Nucleotide Targeter tool (https://tale-nt.cac.cornell.edu/software). *g0s2*-specific TALEN constructs were

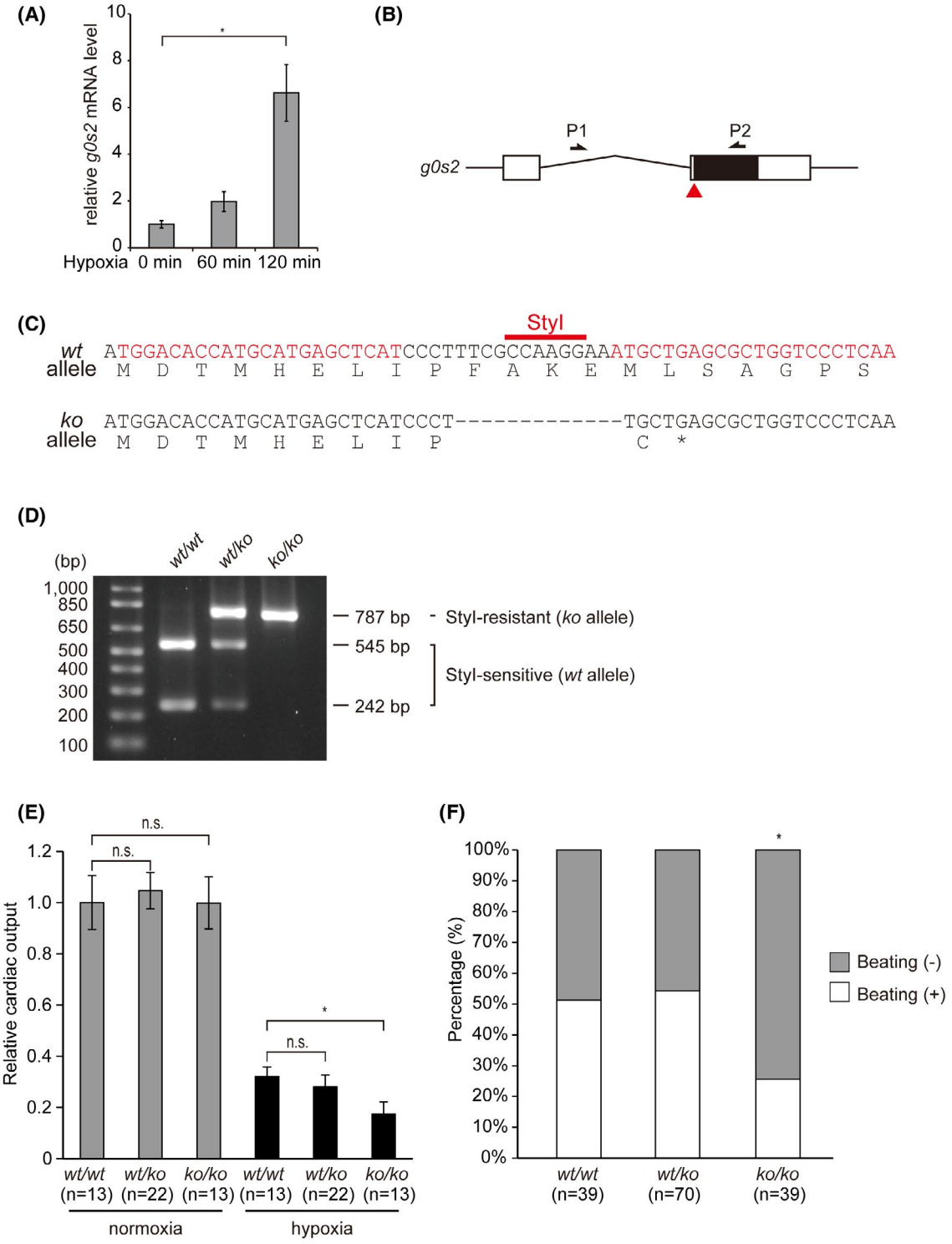

FIGURE 1 Generation of TALEN-mediated G0s2 KO fish and functional assay in a hypoxic stress model. A, qRT-PCR analysis of endogenous *g0s2* in zebrafish larvae exposed to mild hypoxia (5% O_2) for 0, 60, and 120 minutes. Relative *g0s2* mRNA levels were normalized to *actb* mRNA levels, used as an internal control. Data are represented as means ± SEM of three different samples per group. *, $P < .05$. B, Schematic representation of the endogenous *g0s2* locus of zebrafish. The transcription start site in exon 2 is indicated by a red arrowhead. Forward and reverse primer sites are indicated as P1 and P2, respectively. C, Sequence alignment of the TALEN-generated mutant allele (*ko*) for *g0s2*. The 13 residues indicated as bars in the *ko* allele were deleted. TALEN-recognizing sequences are indicated by red letters. * indicates premature stop codon induced by frameshift. The *Sty*I digestion site for RFLP analysis is indicated by a red line. D, RFLP analysis of F2 off spring of *wt/wt*, *wt/ko*, and *ko/ko*. E, Cardiac output (CO) of zebrafish larvae hearts (*wt/wt, wt/ko, ko/ko*) before and after a short period of mild hypoxic exposure (5% O_2 for 30 minutes). The measurements were normalized to the average CO of *wt/wt* under normoxia. Data are represented as means ± SEM *wt/wt*: n = 13, *wt/ko*: n = 22, *ko/ko*: n = 13. *, $P < .05$. n.s., not significant compared to *wt/wt*. F, Percentage of zebrafish larvae hearts (*wt/wt, wt/ko, ko/ko*) that continued beating under mild hypoxia (5% O_2 for 50 minutes). *wt/wt*: n = 39, *wt/ko*: n = 70, *ko/ko*: n = 39. *, $P < .05$ by χ^2 test comparing *wt/wt*, *wt/ko* and *ko/ko*

engineered using the TALEN Golden Gate assembly system described by Cermak et al.[12] The TALEN expression backbones, pCS2TAL3DD and pCS2TAL3RR, and the plasmids providing repeat variable diresidues (RVD) for Golden Gate Cloning were obtained from Addgene (Watertown, MA, USA).

2.3.2 | Microinjection

Forward and reverse TALEN mRNAs (100 pg each) were injected together into the blastomeres of one-cell stage zebrafish embryos. The synthesized mRNAs were dissolved in the injection buffer (40 mM HEPES [pH 7.4], 240 mM

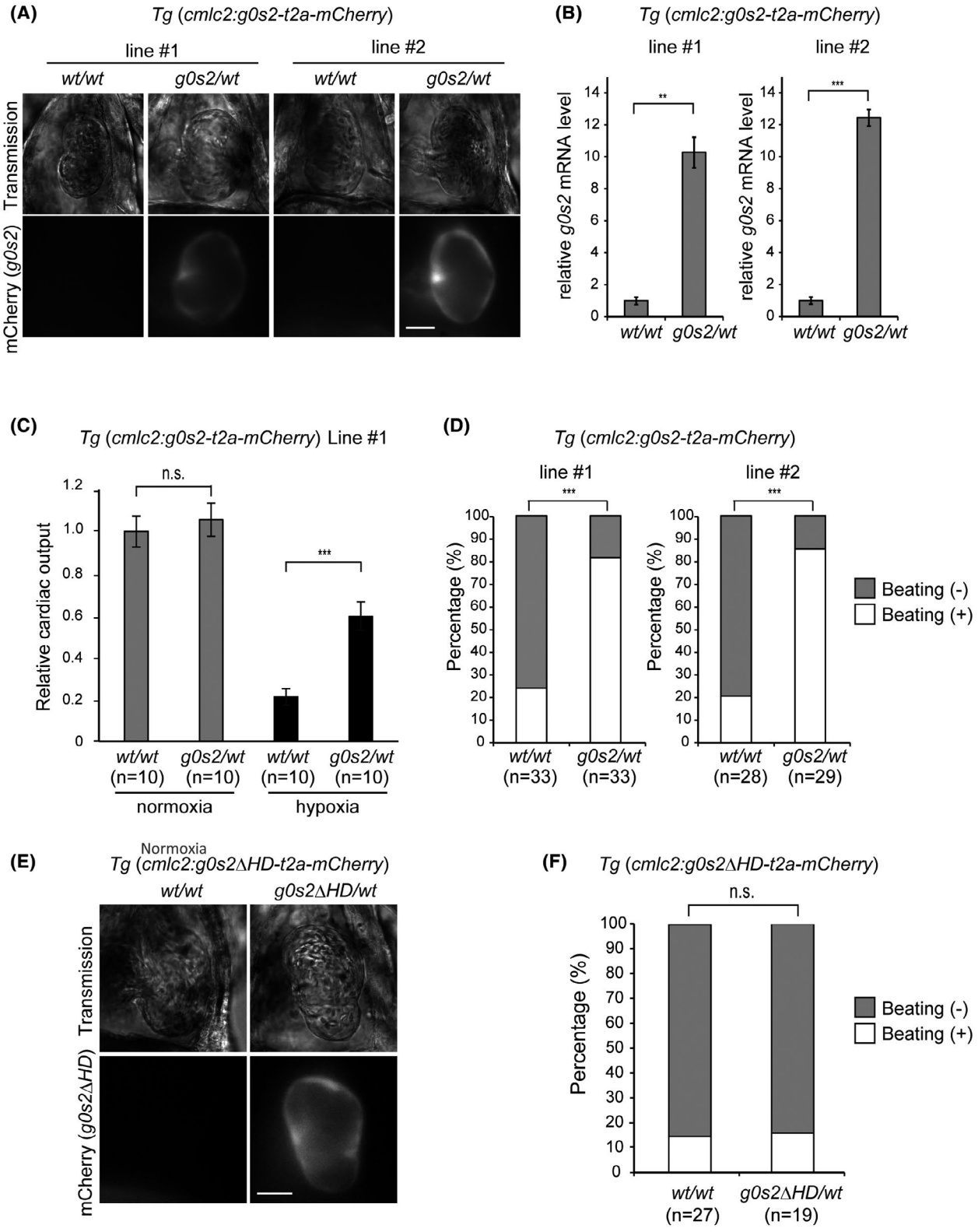

FIGURE 2 Ischemic tolerance in cardiomyocyte-specific G0s2 transgenic zebrafish. A, Representative bright field images (upper panels) and mCherry fluorescence images (bottom panels) of *Tg (cmlc2:g0s2-t2a-mCherry)* zebrafishes. Scale bar, 50 μm. B, qRT-PCR analysis of *g0s2* in *Tg (cmlc2:g0s2-t2a-mCherry)* zebrafish. Total RNA from *g0s2* transgenic (*g0s2/wt*) fish or wild-type littermates (*wt/wt*) from two lines was extracted from 8 to 10 fish at 5 days post-fertilization. Relative *g0s2* mRNA levels were normalized to *actb* mRNA levels, used as an internal control. Data are represented as means ± SEM of three different samples per group. **, $P < .01$. ***, $P < .001$. C, Cardiac output of zebrafish larvae hearts of *g0s2* transgenic fish larvae (*g0s2/wt*) or wild-type littermates (*wt/wt*) in transgenic line #1 before and after short period of mild hypoxic exposure (5% O_2 for 30 minutes). The measurements were normalized to the average CO of *wt/wt* under normoxia. Data are represented as means ± SEM n = 10 in each genotype. ***, $P < .001$. n.s., not significant compared to *wt/wt*. D, Percentage of hearts of *g0s2* transgenic fish larvae (*g0s2/wt*) or wild-type littermates (*wt/wt*) that continued beating under severe hypoxia (3% O_2 50 minutes). *g0s2/wt*; n = 33, *wt/wt*: n = 33 in line #1. *g0s2/wt*: n = 28, *wt/wt*: n = 29 in line #2. ***, $P < .001$ by χ^2 test comparing *g0s2/wt* with *wt/wt*. E, Representative bright field images (upper panels) and mCherry fluorescent images (bottom panels) of *Tg (cmlc2:g0s2-t2a-mCherry)* zebrafish. Scale bar, 50 μm. F, Percentage of hearts of *g0s2*ΔHD transgenic fish larvae (*g0s2ΔHD/wt*) or wild-type littermates (*wt/wt*) that continued beating under severe hypoxia (3% O_2 for 50 minutes). *g0s2ΔHD/wt:* n = 19, *wt/wt*: n = 27. n.s., not significant by χ^2 test comparing *g0s2*ΔHD/*wt* with *wt/wt*

KCl, and 0.5% phenol red). The synthesized mRNA (1 pg) was injected into one-cell stage zebrafish embryos or the yolk syncytial layer (YSL) around high-stage embryos. Injection into the YSL was confirmed by the distribution of co-injected rhodaminedextran (Sigma, St. Louis, MO, USA).

2.3.3 | Founder selection and establishment of *g0s2* KO fish line

High-resolution melting analysis[13] and/or sequence analysis was used to identify founders with little sequence heterogeneity surrounding the target site. F0 fish with TALEN-induced mutations were crossed with WT fish and F1 offspring was sequenced and mutant allele was confirmed. F1 offspring heterozygous for mutant allele with a 13 bp deletion leading a premature stop codon (Figure 1C) were selected. To establish and maintain a mutant line, heterozygous male fish was crossed to the wild-type fish.

2.3.4 | Genotyping of mutant alleles

Total genomic DNA was extracted using KAPA Express Extract Kit (Kappa Biosystems, Wilmington, MA, USA). The genomic DNA was used as template to amplify the *g0s2* TALEN target locus. Primers flanking the target site of *g0s2*:

g0s2 genotype Fw, CTGTGTTTATGTTGAATTGATT TTCCACCTAATCA

g0s2 genotype Rv, CTCCATCACCGCATCCATTTC TTCATCTTCA

To assess *g0s2* mutant alleles, the PCR amplicons were incubated with *Sty*I (New England Biomedical, South Weymouth, MA, USA) at 37°C for 6 hours, resulting in the generation of 545 bp and 242 bp fragments. Mutant allele was detected by loss of the restriction recognition site by *Sty*I and the presence of undigested band of 683 bp (Figure 1D).

2.3.5 | Generation of transgenic zebrafish line expressing *g0s2-t2a-mCherry* in the heart

We co-injected pT2A/*cmlc2:g0s2-t2a-mCherry* construct with Tol2 mRNA into fertilized eggs of wild-type fish. F0 embryos showing strong mCherry expression were selected and were crossed with wild-type fish. F1 embryos that showed the brightest mCherry expression were raised to establish *Tg* (*cmlc2:g0s2-t2a-mCherry*) zebrafish.

2.3.6 | Generation of transgenic zebrafish line expressing Mit-ATeam in the heart

A transgenic zebrafish line expressing the Mit-ATeam specifically in heart was generated by the Gal4-UAS system-based method as described previously.[14] Briefly, we co-injected 5xUAS-Mit-ATeam construct with Tol2 mRNA into fertilized eggs of hspGFF3A fish expressing Gal4 in heart. F0 embryos showing strong mosaic CFP expression were selected and were crossed with wild-type fish. F1 embryos that showed the brightest CFP expression were raised to establish *Tg (hspGFF3A:Gal4, UAS: Mit-ATeam)* fish. ATeam RK fish was also generated using a construct with a control ATP sensor named ATeam1.03$^{R122K/R126/K}$ that lacks ATP binding capacity.

2.3.7 | In vivo real-time ATP imaging in a zebrafish beating heart

A larvae at 4 or 5 dpf was placed in a tiny well made with agarose gel (2.0%) containing tricaine (0.16 mg/mL) on a glass-bottomed dish and was viewed ventrally by the inverted microscope (Olympus IX81). The fishes were maintained on a microscope at 28°C using a stage-top incubator (Tokai Hit, Fujinomiya, Shizuoka, Japan). Fishes were illuminated using CoolLED pE-1 excitation system (CoolLED, Andover, Hampshire, UK) with a wavelength of 425 nm. Fluorescence of Mit-ATeam in zebrafish heart was collected with a silicon

oil immersion objective (X30 Olympus, NA 1.05; Olympus, Shinjuku, Tokyo, Japan) and imaged by a dual cooled charge-coupled device (CCD) camera (ORCA-D2; Hamamatsu Photonics, Hamamatsu, Shizuoka, Japan) with a dichroic mirror 510 nm and two emission filters (483/32 nm for CFP and 542/27 nm for YFP; A11400-03, Hamamatsu Photonics, Hamamatsu, Shizuoka, Japan). Exposure time of each frame was 20 ms. For the control of oxygen concentration during time-lapse imaging, digital gas mixer for stage-top incubator GM8000 (Tokai Hit, Fujinomiya, Shizuoka, Japan) was used to create hypoxic (3% O_2 as severe hypoxia or 5% O_2 as mild hypoxia) and normoxic (20%) conditions. Image analysis was performed using MetaMorph (Molecular Devices, San Jose, CA, USA). The YFP/CFP emission ratio was calculated by dividing pixel-by pixel an YFP image with a CFP image after background subtraction.

2.3.8 | Cardiac "mosaic" overexpression of *g0s2* in Mit-ATeam transgenic zebrafish

We generated the construct that zebrafish *g0s2* was fused to self-cleaving peptide T2A[15] and mCherry placed downstream of cardiac myosin light chain 2 promoter (pT2A/*cmlc2:g0s2-t2a-mCherry*). Tol2 mRNA was co-injected with pT2A/*cmlc2:g0s2-t2a-mCherry* into Mit-ATeam transgenic line embryos to increase mosaicism.[14]

2.4 | Measurement of cardiac function

Zebrafish larvae are mounted at prone position with low-melting point agarose in glass bottom dish. Dish are placed in the stage top incubator and oxygen controller GM8000 (Tokai Hit, Fujinomiya, Shizuoka, Japan). Heart rates (HR) were measured under inverted microscope (Olympus IX81; Olympus, Shinjuku, Tokyo, Japan) for 10 seconds. The continuation of cardiac contraction was assessed after 50 minutes exposure to hypoxia (3% O_2 as severe hypoxia and 5% O_2 as mild hypoxia). Cardiac output (CO) was assessed before and after exposure to a short period (30 minutes) of hypoxia (5% O_2). We acquired movies of beating zebrafish heart with frame rate of 20 frames per second, sampling ventricular end-diastolic volume (EDV) and ventricular end-systolic volume (ESV) as described previously.[16] CO was calculated from EDV, ESV, and HR as follows: $CO = (EDV - ESV) \times HR$

2.4.1 | Confocal microscopy

After treated with 50 nM of Mitotracker Red for 4 hours, cultured zebrafish cardiomyocytes were imaged by FV1000D confocal microscope using a PL APO 60X, 1.35 NA, oil immersion objective lens (Olympus, Shinjuku, Tokyo, Japan).

2.4.2 | Animals

All procedures were performed in conformity with the Guide for the care and use of laboratory animals (NIH publication no. 85-23, revised 1996) and were approved by the Osaka University Committee for Laboratory Animal Use.

2.4.3 | Statistical analyses

Our data are expressed as means ± SEM of at least three independent experiments. The two-tailed Student's *t*-test was used to analyze differences between two groups unless otherwise noted. $P < .05$ was considered statistically significant.

3 | RESULTS

3.1 | Generation of zebrafish harboring TALEN-mediated *g0s2* KO

Before examining the in vivo protective role of G0s2, we first investigated whether the expression of endogenous *g0s2* is induced under hypoxic conditions in animal models as well as it is in NRVCs. When zebrafish larvae were exposed to mild hypoxic condition (5% O_2), the mRNA expression level of *g0s2* immediately increased (Figure 1A), suggesting that G0s2 plays a role in adapting to hypoxic conditions. For loss-of-function experiments, we generated *g0s2* knockout (KO) zebrafish using TALEN. The TALEN target site was designed against exon 2, which includes the coding sequence (Figure 1B). F0 embryos injected with TALEN mRNAs were grown to adulthood. We crossed F0 fish with wild-type fish, screened F1 offspring by sequence analysis, and confirmed germline-transmitted mutant alleles. Among them, we chose founder fish with *g0s2*-edited allele with a 13-bp deletion (*ko* allele) leading to a premature stop codon (Figure 1C) to generate the *g0s2* KO zebrafish line. Genotyping was confirmed by restriction fragment length polymorphism (RFLP) analysis (Figure 1D). Heterozygous mutant fish were crossed to obtain homozygous mutants. The expected Mendelian ratios were observed, indicating no embryonic lethality due to loss of *g0s2*. No overt phenotype was observed that co-segregated with the *ko* allele during development and growth.

3.2 | *g0s2* KO zebrafish hearts had significantly lower tolerance to hypoxic stress than wild-type and heterozygous *g0s2* mutant zebrafish

We next examined the in vivo protective role of G0s2 against hypoxia. Zebrafish larvae generated by crossing heterozygous *g0s2* KO males and females were used for this experiment. We compare the cardiac output (CO)[16] after a short (30 minutes) hypoxic exposure (cardiac function assay) and the percentage of hearts that still continued beating even after prolonged (50 minutes) hypoxic exposure (beating assay). It should be noted that the genotype was confirmed by RFLP after completion of the hypoxic experiment to prevent bias when collecting data. There was no difference in CO among genotypes before exposure to hypoxia (Figure 1E). However, the hearts of homozygous *g0s2* mutants had significantly lower CO in the cardiac function assay after a short hypoxic exposure (Figure 1E), and a significantly lower percentage of hearts that still continued beating after prolonged hypoxic stress, than the wild-type and heterozygous mutants (Figure 1F). Together, consistent with the cellular experiments, these data indicate that endogenous *g0s2* preserved tissue function under hypoxic stress in zebrafish hearts.

3.3 | Cardiomyocyte-specific *g0s2* transgenic zebrafish had significantly greater tolerance to hypoxic stress than wild-type zebrafish

We next generated cardiomyocyte-specific *g0s2* transgenic zebrafish to examine the effect of overexpressed *g0s2*. Two zebrafish lines stably expressing *g0s2* in the whole heart were produced (Figure 2A). The *g0s2* expression levels in these transgenic lines were approximately 10-fold higher than the endogenous expression level in wild-type fish (Figure 2B). We performed the cardiac function and beating assays in this gain-of-function model. First, we exposed cardiomyocyte-specific *g0s2* transgenic zebrafish to short period of mild hypoxia (5% O_2 for 30 minutes) and compared their CO with that of wild-type littermates. CO of cardiomyocyte-specific *g0s2* transgenic zebrafish was significantly higher after hypoxic exposure, although there was no difference under normoxia (Figure 2C). For the beating assay, we exposed fish to severe hypoxia (3% O_2 for 50 minutes) to examine the protective role of overexpressed *g0s2*. In this model, most of the wild-type littermate zebrafish hearts stopped beating at the end of the exposure period (3% O_2 for 50 minutes). On the other hand, the hearts of both transgenic lines exhibited significantly greater tolerance of hypoxic stress than those of their wild-type littermates (Figure 2D).

In our previous report, we showed that G0s2 interacts with F_oF_1-ATP synthase via its HD, and that a G0s2 deletion mutant lacking the HD (G0s2ΔHD) loses its function.[7] Therefore, we also established a transgenic zebrafish line stably expressing mutant G0s2 without the HD (*g0s2*ΔHD) (Figure 2E). In contrast to full-length *g0s2* transgenic fish, the hearts of *g0s2*ΔHD transgenic fish did not exhibit any protective effect against hypoxia (Figure 2F).

Collectively, these results suggested that overexpression of *g0s2* protects cardiac function during hypoxic stress.

3.4 | Generation of Mit-ATeam transgenic zebrafish

Next, we tried to establish an in vivo ATP imaging system in beating zebrafish hearts. For this purpose, we established a Gal4 transgenic zebrafish line (Mit-ATeam zebrafish) that specifically expresses Mit-ATeam in cardiomyocytes (Figure 3A). Confocal microscopy confirmed that Mit-ATeam correctly localized to mitochondria in the heart (Figure 3B,C). During in vivo ATP imaging, we observed only slight changes in the YFP/CFP ratio from the diastolic to systolic phase of the beating heart, indicating that motion artifacts in this assay were minimal (Figure 3D-F). We next validated our in vivo ATP imaging system using ATP synthase inhibitor (oligomycin A) and uncoupler (FCCP). Both 10 μg/mL of oligomycin A and 10 μM of FCCP significantly decreased YFP/CFP ratio of Mit-ATeam fluorescence as expected (Figure 3G). Thus, we could successfully visualize intra-mitochondrial ATP concentrations ($[ATP]_{mito}$) in in vivo beating hearts with minimal artifacts.

3.5 | Visualization of ATP dynamics in zebrafish heart during hypoxia and re-oxygenation

Using Mit-ATeam zebrafish, we successfully observed the decline of $[ATP]_{mito}$ under hypoxia and subsequent recovery of $[ATP]_{mito}$ following re-oxygenation (Figure 4A,C).

We also generated transgenic zebrafish expressing ATeam RK, a control FRET probe that cannot bind to ATP, to exclude possible imaging artifacts induced by hypoxic conditions (eg, acidosis). The YFP/CFP ratio of ATeam RK fish was constant during hypoxia and re-oxygenation, corroborating the idea that the change in the FRET signal observed in Mit-ATeam fish reflected a genuine change in $[ATP]_{mito}$ (Figure 4B,C).

These findings demonstrate that we successfully established a method for visualizing $[ATP]_{mito}$ during hypoxia and re-oxygenation.

3.6 | Cardiomyocyte-specific *g0s2* transgenic zebrafish have significantly higher $[ATP]_{mito}$ during hypoxia and re-oxygenation

Next, we compared the ATP dynamics of cardiomyocyte-specific *g0s2* transgenic zebrafish with that of wild-type littermate controls and *g0s2*ΔHD transgenic fish. After crossing with Mit-ATeam fish, we visualized and compared $[ATP]_{mito}$ during hypoxia and re-oxygenation among genotypes. In cardiomyocyte-specific *g0s2* transgenic zebrafish, $[ATP]_{mito}$ was significantly higher than that of control littermates under hypoxia, whereas there was no difference between *g0s2*ΔHD transgenic

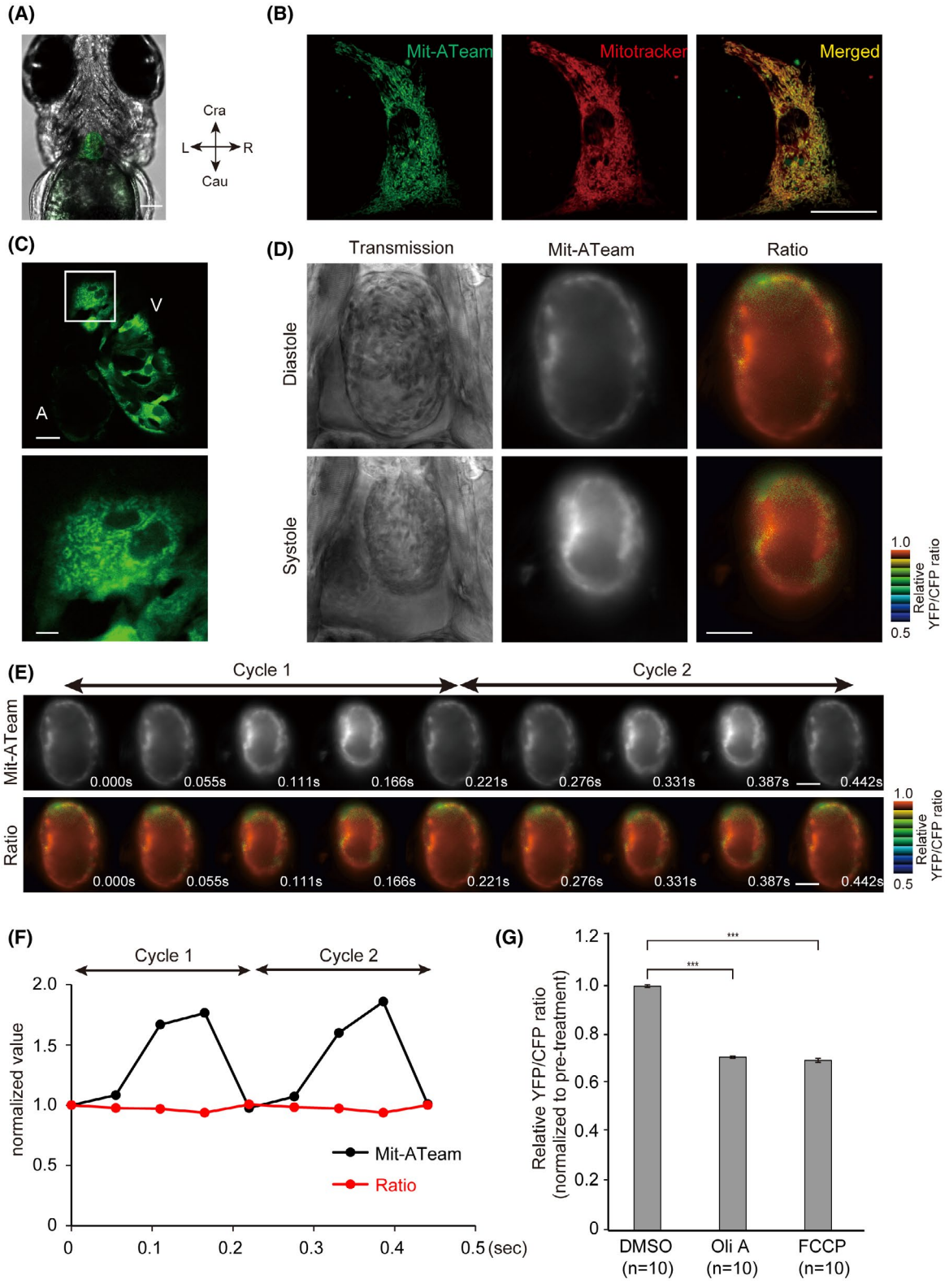

FIGURE 3 Establishment of in vivo ATP imaging system using Mit-ATeam zebrafish. A, Transgenic zebrafish (*hspGFF3A:Gal4, UAS:Mit-ATeam*. ie, Mit-ATeam zebrafish) at 4 days post-fertilization. An image of Mit-ATeam fluorescence (green) was imposed on a transmission image (grey). Cra, cranial; Cau, caudal; L, left; R, right. Scale bar, 100 μm. B, Mit-ATeam localizes to mitochondria of cultured zebrafish adult cardiomyocytes. Mitochondria were labeled with Mitotracker Red. Dashed line indicates cell contours. Scale bar, 10 μm. C, Confocal image of the whole heart (upper panel) of a live Mit-ATeam zebrafish. The white-boxed region in the upper panel is enlarged and shown below. V, ventricle; A, atrium. Scale bars, 20 μm (upper panel) and 5 μm (lower panel). D, Diastolic and systolic bright-field images (left), Mit-ATeam fluorescence images (middle), and YFP/CFP ratiometric pseudo-colored images (right) of a Mit-ATeam zebrafish heart. Scale bar, 50 μm. E, Representative sequential YFP/CFP ratiometric pseudo-colored images of Mit-ATeam fluorescence in Mit-ATeam zebrafish in cardiac cycle. Scale bar, 50 μm. F, YFP/CFP emission ratio plots (red) and intensity plots (black) of Mit-ATeam fluorescence in cardiac cycle. Circular regions of interest (ROI) were manually registered in each frame as shown in (E) and the average YFP/CFP ratio and intensity of Mit-ATeam fluorescence within each ROI were plotted. The measurements were normalized against the value at time point 0 in each fish. G, Relative YFP/CFP ratio (Post-treatment/Pre-treatment) of Mit-ATeam after DMSO (control) or OXPHOS inhibitors. Data are represented as means ± SEM (n = 10). ***, $P < .001$ compared to DMSO. DMSO, dimethyl sulfoxide; Oli A, oligomycin A; FCCP, trifluoromethoxy carbonylcyanide phenylhydrazone

fish and control fish (Figure 5A,B). These findings suggested that overexpression of *g0s2* attenuates the decrease in mitochondrial ATP production even under hypoxia.

3.7 | Mosaic overexpression model of *g0s2* confirms that G0s2 preserves cardiac function under hypoxia by maintaining $[ATP]_{mito}$

To confirm the mechanism by which G0s2 preserves cardiac function under hypoxia, we used Mit-ATeam zebrafish to investigate whether the *g0s2*-overexpressed region could maintain ATP production during hypoxia. For this purpose, we established a mosaic *g0s2* overexpression model in the Mit-ATeam zebrafish heart. This system enabled us to compare the contraction and ATP dynamics between *g0s2*-expressing and non-expressing cardiomyocytes side-by-side in a same heart. To visualize *g0s2* expression via mCherry fluorescence, we designed a construct encoding a zebrafish *g0s2* with cardiomyocyte-specific promoter followed by the mCherry reporter with the 2A self-cleaving peptide[15] (Figure 6A left). We then injected the DNA construct into fertilized eggs of Mit-ATeam zebrafish (Figure 6A middle). It should be noted that *g0s2* was expressed in a mosaic pattern (Figure 6A right). The *g0s2* overexpression level in this model was approximately fourfold higher than that of endogenous *g0s2* (Figure 6B). Again, this mosaic expression model of *g0s2* allowed us to observe real-time $[ATP]_{mito}$ changes and cardiac function of both types of cardiomyocytes (ie, *g0s2*-overexpressing and control) simultaneously within the heart of a single fish, thereby eliminating interference due to individual differences between fish. Even under normoxic conditions, the *g0s2*-overexpressing region (mCherry-positive) contained higher $[ATP]_{mito}$ than the control region (mCherry-negative) (Figure 6C), suggesting that *g0s2* enhances ATP production in normoxia as well. During hypoxia and subsequent re-oxygenation, the *g0s2*-overexpressing region exhibited a slower decline and faster recovery of $[ATP]_{mito}$ than the control region (Figures 6D,E). In contrast, regional overexpression of *g0s2ΔHD* did not affect $[ATP]_{mito}$ (Figure S1). Regarding cardiac function, we observed that ventricular wall motion and heart rate decreased in parallel with the decrease in $[ATP]_{mito}$ during hypoxia, as expected (Figure 6F; Supporting Information Movie S1). Very importantly, the *g0s2*-overexpressing region exhibited preserved wall motion under the hypoxic conditions, whereas the control region exhibited a paradoxical outward systolic bulging that is also observed in the severest ischemic myocardium in clinical cardiology (termed "dyskinesis")[17,18] (Figure 6F middle panel; Supporting Information Movie S1). Furthermore, after subsequent re-oxygenation, ventricular wall motion was partially restored with concomitant recovery of $[ATP]_{mito}$, and there was no difference in ventricular wall motion between these two regions (Figures 6F right panel; Supporting Information Movie S1). These results clearly demonstrated that *g0s2* expression preserves cardiac function during hypoxia by maintaining ATP production in a cell-autonomous manner.

4 | DISCUSSION

In this study, using zebrafish harboring TALEN-mediated *g0s2* KO zebrafish and cardiomyocyte-specific *g0s2* transgenic fish, we demonstrated that G0s2 protects cardiac function under hypoxic energy crisis. Additionally, the in vivo real-time ATP imaging system showed that overexpressed *g0s2* protects cardiac function by preserving mitochondrial ATP production.

As the most metabolically active organ, the heart has the highest content of mitochondria.[19,20] Therefore, the function of the heart strongly depends on mitochondrial ATP production by OXPHOS. In cultured cells, a metabolic switch from mitochondrial OXPHOS to glycolysis has been widely known.[21-23] However, even in limited oxygen concentrations, OXPHOS activity appears to be essential, as glycolytic ATP production alone is not enough to maintain energy homeostasis in highly metabolically active organs like heart.[5] Here, we demonstrated that G0s2

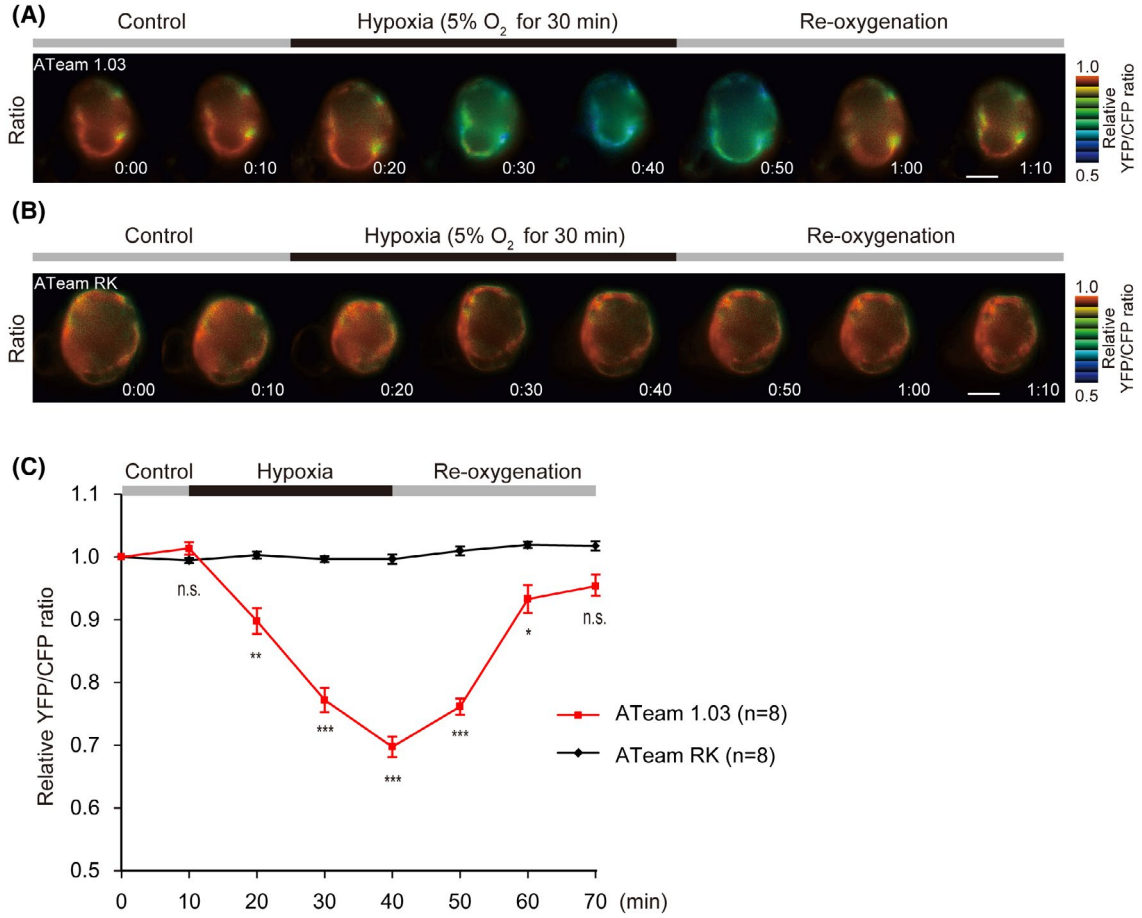

FIGURE 4 In vivo ATP imaging during hypoxia and re-oxygenation. A, Representative sequential YFP/CFP ratiometric pseudo-colored images of Mit-ATeam fluorescence in Mit-ATeam zebrafish during mild hypoxia (5% O_2 for 30 minutes) and re-oxygenation (20% O_2 for 30 minutes). Scale bar, 50 μm. B, Representative sequential YFP/CFP ratiometric pseudo-colored images of a control ATP sensor named ATeam1.03$^{R122K/R126/K}$ that lacks ATP binding capacity during hypoxia (5% O_2 for 30 minutes) and re-oxygenation (20% O_2 for 30 minutes). Scale bars, 50 μm. C, YFP/CFP emission ratio plots of Mit-ATeam and ATeam RK fluorescence during hypoxia (5% O_2 for 30 minutes) and re-oxygenation (20% O_2 for 30 minutes). The measurements were normalized against the ratio at time point 0 in each fish and compared between Mit-ATeam and ATeam RK at each time point. Data are represented as means ± SEM (n = 8). *, $P < .05$ **, $P < .01$. ***, $P < .001$ comparing to Mit-ATeam and ATeam RK

maintains mitochondrial ATP production and protects tissue function under hypoxia when oxygen supply is limited, but not completely shut off. Although the proton motive force (PMF) generated by mitochondrial respiratory chain complexes decreases under hypoxia,[24] G0s2 may improve the efficiency of ATP production with equivalent PMF. Indeed, we showed that *g0s2*-expressing cardiomyocyte populations exhibited increased $[ATP]_{mito}$ both in normoxia and hypoxia (Figure 6C). Notably in this regard, all cardiomyocytes in the heart were exposed to the same degree of hypoxia, and PMF was probably also reduced to the same extent in this mosaic overexpression model (Figure 6A). Collectively, our findings indicate that G0s2 enhances mitochondrial ATP production with equivalent PMF and acts as a guardian of hypoxic tissue.

From a clinical standpoint, it is widely known that a short period of ischemia strongly protects tissue against damage from subsequent prolonged ischemia (ie, preconditioning-induced ischemic tolerance).[25] Indeed, ATP loss during oxygen deprivation is slower in ischemic preconditioned tissue than in normal tissue.[26] Therefore, G0s2 may be involved in this strong intrinsic cell-protective effect although further studies using large animals are necessary.

Several reports have shown that G0s2 is a multifaceted protein involved in proliferation, apoptosis, inflammation, lipid metabolism, and carcinogenesis.[27] Although it remains unclear how G0s2 distinguishes these multiple functions in different cells and tissues is still not clear, the cell- and tissue-specific responses of mRNA and protein expression against various stresses such as hypoxia and fasting may be a clue for the cell- and tissue-specific roles of G0s2. So far, the in vivo function of G0s2 has mainly been examined in adipose tissue and liver using transgenic mice[28] and G0s2-null mice.[29,30] These studies suggested

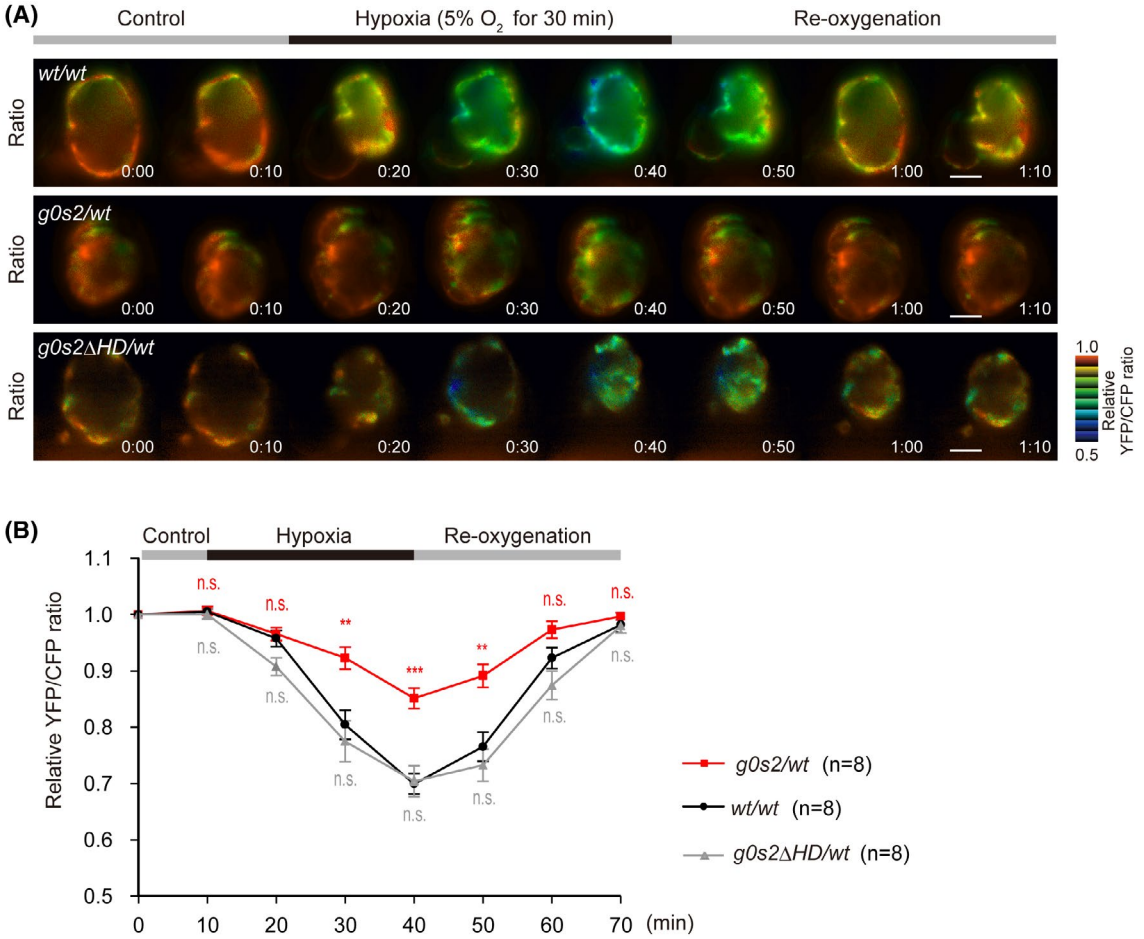

FIGURE 5 In vivo ATP imaging in cardiomyocyte-specific *g0s2* transgenic zebrafish. A, Representative sequential YFP/CFP ratiometric pseudo-colored images of Mit-ATeam fluorescence in cardiomyocyte-specific *g0s2* transgenic zebrafish during mild hypoxia (5% O_2 for 30 minutes) and re-oxygenation (20% O_2 for 30 minutes). Scale bar, 50 μm. B, YFP/CFP emission ratio plots of Mit-ATeam fluorescence in cardiomyocyte-specific *g0s2* transgenic zebrafish. The measurements were normalized against the ratio at time point 0 in each fish and compared between *g0s2/wt* and *wt/wt* (red) and between *g0s2ΔHD/wt* vs *wt/wt* (gray) at each time point. Data are represented as means ± SEM (n = 8). **, $P < .01$. ***, $P < .001$ compared to *wt/wt*

that G0s2 functions as an inhibitor of adipose triglyceride lipase (ATGL), the rate-limiting triglyceride hydrolase and enhances lipid accumulation in adipose tissue and liver. However, other functions of G0s2 (ie, ATGL-independent functions) have not been examined in vivo. Although we cannot exclude the possibility that altered lipid metabolism in liver and adipose tissue indirectly influence cardiac phenotypes in the global *g0s2* KO model, the cardiomyocyte-specific and mosaic overexpression models demonstrated that G0s2 protects the heart from hypoxic stress in a cell-autonomous manner.

Another interesting aspect of this study is the establishment of a system for in vivo imaging of mitochondrial ATP production in a beating zebrafish heart. Reliable measurements of highly labile metabolites including ATP from extracted tissues are very difficult.[31] Therefore, in vivo real-time metabolic imaging is needed for the investigations of energy metabolism along with in vivo tissue function. For this purpose, we introduced the ATP-sensing FRET biosensor Mit-ATeam[6,32] into zebrafish heart and successfully established a Mit-ATeam zebrafish line. It should be noted that the heart is an ideal tissue for ATP imaging because we can simultaneously evaluate tissue function (ie, contraction of the heart muscle) as well as ATP dynamics. In other words, using Mit-ATeam zebrafish, we can simultaneously assess mitochondrial ATP production and cardiac function. This in vivo imaging system should be useful for the investigation of diseases related to energy metabolism such as ischemic heart diseases, cardiomyopathies, and metabolic diseases.[33]

Taken together, our results show that G0s2 works to maintain mitochondrial ATP production and tissue function, even under hypoxic conditions. Enhancing the expression level and/or function of G0s2 could be beneficial for the treatment of hypoxia-related disorders such as ischemic heart disease.

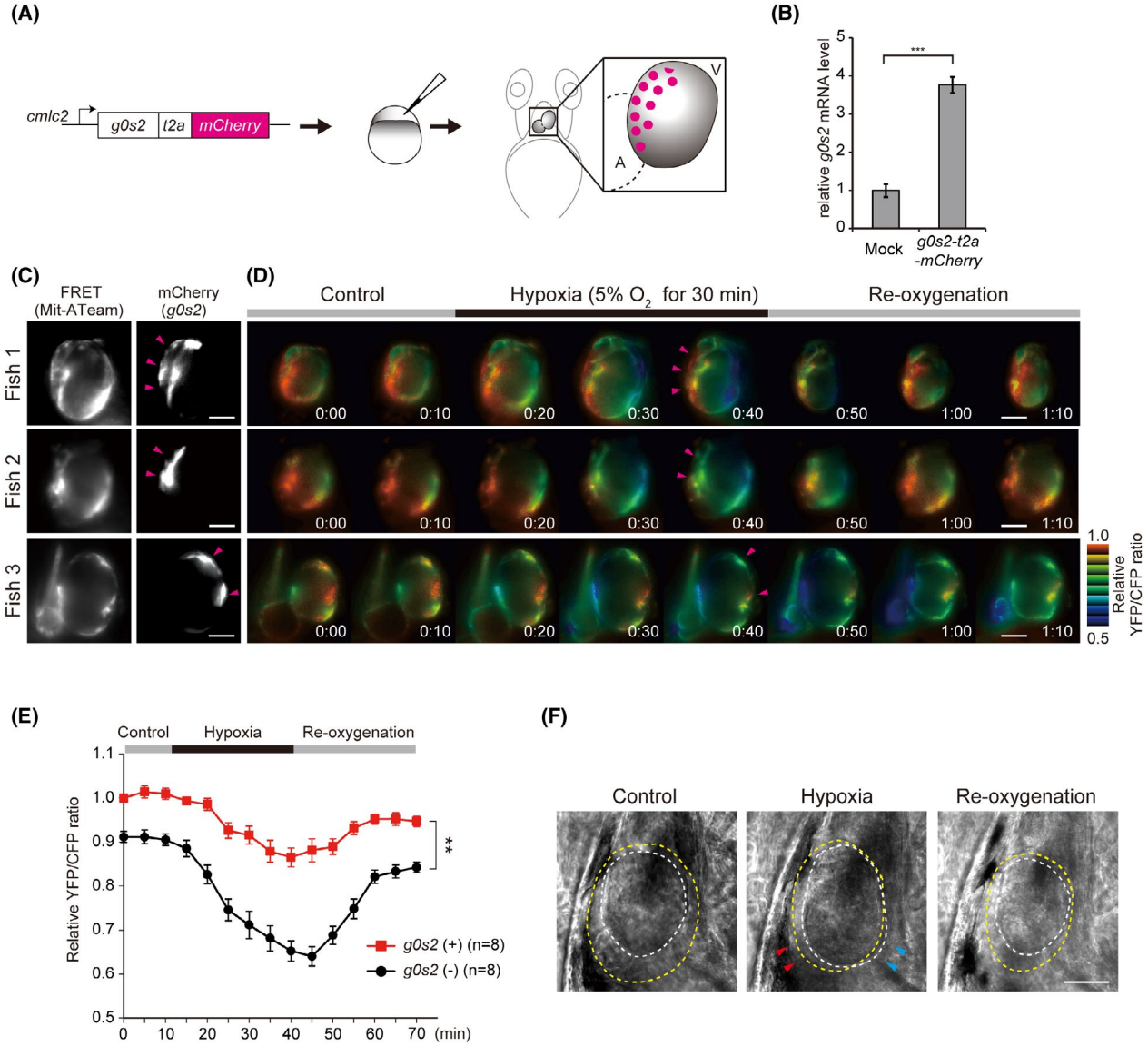

FIGURE 6 Regional overexpression of G0s2 rescues cardiac dysfunction under hypoxia. A, Schematic representation of a zebrafish model that allows the assessment of the in vivo role of G0s2. The cardiac myosin light chain 2 promoter-driven zebrafish *g0s2* DNA construct (*cmlc2*:*g0s2-t2a-mCherry*) was injected into the one-cell stage embryo of Mit-ATeam zebrafish. A scheme of the injected larvae is shown. Note that the injected *g0s2* is mosaically expressed in the heart (red spots, shown in enlarged panel on the right). V, ventricle; A, atrium. B, qRT-PCR analysis of *g0s2* mRNA expression in a mosaic overexpression model of G0s2. Mock or *cmlc2:g0s2-t2a-mCherry* plasmid was injected into one-cell stage embryos of Mit-ATeam zebrafish. Total RNA was extracted from 8-10 fish at 5 days post-fertilization. Relative *g0s2* mRNA levels were normalized to *actb* mRNA levels, used as an internal control. Data are represented as means ± SEM of three different samples per group. ***, $P < .001$. C, Representative fluorescence wide-field images of Mit-ATeam zebrafish mosaically expressing *g0s2*. Fluorescence images of Mit-ATeam (left) and mCherry (*g0s2*) (right) are shown. Red arrowheads indicate *g0s2*-expressing regions. Scale bars, 50 μm. D, Sequential YFP/CFP ratiometric pseudo-colored images of Mit-ATeam fluorescence in Mit-ATeam zebrafish in (C) during mild hypoxia (5% O_2 for 30 minutes) and re-oxygenation (20% O_2 for 30 minutes). Red arrowheads indicate *g0s2*-expressing regions. Scale bars, 50 μm. E, YFP/CFP emission ratio plots of Mit-ATeam fluorescence of *g0s2*-expressing [*g0s2* (+)] and control [*g0s2* (−)] regions during hypoxia and re-oxygenation. The measurements were normalized against the ratio of *g0s2* (+) region at time 0 in each fish. Data are represented as means ± SEM (n = 8). Data were collected from eight fish including the three fish in (C), by drawing a ROI within *g0s2* (+) (n = 8) and *g0s2* (−) (n = 8) regions in each fish. **, $P < .01$ by repeated measured ANOVA (analysis of variance) comparing *g0s2* (+) with *g0s2* (−) region. F, End-systolic bright field images of the Fish1 heart in (C and D) under control conditions (20% O_2), mild hypoxia (5% O_2 for 30 minutes), and subsequent re-oxygenation (20% O_2 for 30 minutes). The white dashed lines indicate the ventricular surface at the end-systolic phase. The yellow dashed lines indicate the ventricular surface at the end-diastolic phase. The red arrowheads indicate the *g0s2* overexpressing region, which exhibited preserved systolic function even under hypoxia. The blue arrowheads indicate the control region, which exhibited a paradoxical outward systolic bulging (ie, dyskinesis; a characteristic wall motion abnormality observed in the severest ischemic myocardium). Scale bar 50 μm. See also Supporting Information Movie S1

ACKNOWLEDGMENT

This research was supported by JSPS KAKENHI Grant Number JP16K09501 and JP19K08581 (to H. Kioka), AMED under Grant Number JP19ek0109412h0001 (to H. Kioka), and JST CREST Grant Number JPMJCR14M2 (to S.T). This research was also supported by grants from the Japan Heart Foundation, Japan Cardiovascular Research Foundation, Japan Research Promotion Society for Cardiovascular Diseases, Japan Medical Association, Takeda Science Foundation, Takeda Medical Research Foundation, Heart Foundation/Novartis Grant for Research Award on Molecular and Cellular Cardiology, Naito Foundation, Banyu Foundation, and Nakatani Foundation. We thank K. Kawakami, R. Fukuda, and National BioResource Project from the Ministry of Education, Culture, Sports, Science, and Technology of Japan for providing plasmid constructs and crucial lines of zebrafish. We thank T. Yoshida and H. Miyagi (Olympus Corporation) for technical advice regarding microscope; S. Ikezawa and M. Kishimoto for technical assistance; Y. Okada, Y. Kurokawa, and H. Kawasaki for secretarial support.

CONFLICT OF INTEREST

The authors declare that they have no conflict of interest.

AUTHOR CONTRIBUTIONS

H. Kioka, Y. Asano, and S. Takashima conceptualized the study. S. Yamazaki and H. Imamura developed the methodology. H. Kioka, H. Kato, and T. Fujita performed investigation. H. Kioka wrote the original draft. Y. Shintani, O. Tsukamoto, M. Kogo, Y. Sakata, and S. Takashima reviewed and edited the manuscript. H. Kioka, Y. Asano, M. Kitakaze, and S. Takashima acquired funding. All authors reviewed and approved the final version of the manuscript.

REFERENCES

1. Chen YC, Taylor EB, Dephoure N, et al. Identification of a protein mediating respiratory supercomplex stability. *Cell Metab*. 2012;15:348-360.
2. Fukuda R, Zhang H, Kim JW, Shimoda L, Dang CV, Semenza GL. HIF-1 regulates cytochrome oxidase subunits to optimize efficiency of respiration in hypoxic cells. *Cell*. 2007;129:111-122.
3. Strogolova V, Furness A, Robb-McGrath M, Garlich J, Stuart RA. Rcf1 and Rcf2, members of the hypoxia-induced gene 1 protein family, are critical components of the mitochondrial cytochrome bc1-cytochrome c oxidase supercomplex. *Mol Cell Biol*. 2012;32:1363-1373.
4. Ritterhoff J, Tian R. Metabolism in cardiomyopathy: every substrate matters. *Cardiovasc Res*. 2017;113:411-421.
5. Brown DA, Perry JB, Allen ME, et al. Expert consensus document: Mitochondrial function as a therapeutic target in heart failure. *Nat Rev Cardiol*. 2017;14:238-250.
6. Imamura H, Nhat KP, Togawa H, et al. Visualization of ATP levels inside single living cells with fluorescence resonance energy transfer-based genetically encoded indicators. *Proc Natl Acad Sci USA*. 2009;106:15651-15656.
7. Kioka H, Kato H, Fujikawa M, et al. Evaluation of intramitochondrial ATP levels identifies G0/G1 switch gene 2 as a positive regulator of oxidative phosphorylation. *Proc Natl Acad Sci USA*. 2014;111:273-278.
8. Hayashi T, Asano Y, Shintani Y, et al. Higd1a is a positive regulator of cytochrome c oxidase. *Proc Natl Acad Sci USA*. 2015;112:1553-1558.
9. DeBerardinis RJ, Thompson CB. Cellular metabolism and disease: what do metabolic outliers teach us? *Cell*. 2012;148:1132-1144.
10. Turner DA, Foster KA, Galeffi F, Somjen GG. Differences in O2 availability resolve the apparent discrepancies in metabolic intrinsic optical signals in vivo and in vitro. *Trends Neurosci*. 2007;30:390-398.
11. Seguchi O, Takashima S, Yamazaki S, et al. A cardiac myosin light chain kinase regulates sarcomere assembly in the vertebrate heart. *J Clin Invest*. 2007;117:2812-2824.
12. Cermak T, Doyle EL, Christian M, et al. Efficient design and assembly of custom TALEN and other TAL effector-based constructs for DNA targeting. *Nucleic Acids Res*. 2011;39:e82.
13. Dahlem TJ, Hoshijima K, Jurynec MJ, et al. Simple methods for generating and detecting locus-specific mutations induced with TALENs in the zebrafish genome. *PLoS Genet*. 2012;8:e1002861.
14. Asakawa K, Suster ML, Mizusawa K, et al. Genetic dissection of neural circuits by Tol2 transposon-mediated Gal4 gene and enhancer trapping in zebrafish. *Proc Natl Acad Sci USA*. 2008;105:1255-1260.
15. Szymczak AL, Vignali DA. Development of 2A peptide-based strategies in the design of multicistronic vectors. *Expert Opin Biol Ther*. 2005;5:627-638.
16. Hoage T, Ding Y, Xu X. Quantifying cardiac functions in embryonic and adult zebrafish. *Methods Mol Biol*. 2012;843:11-20.
17. Sicari R, Cortigiani L. The clinical use of stress echocardiography in ischemic heart disease. *Cardiovasc Ultrasound*. 2017;15:7.
18. Picard MH, Adams D, Bierig SM, et al. American Society of Echocardiography recommendations for quality echocardiography laboratory operations. *J Am Soc Echocardiog*. 2011;24:1-10.
19. Barth E, Stammler G, Speiser B, Schaper J. Ultrastructural quantitation of mitochondria and myofilaments in cardiac muscle from 10 different animal species including man. *J Mol Cell Cardiol*. 1992;24:669-681.
20. Schaper J, Meiser E, Stammler G. Ultrastructural morphometric analysis of myocardium from dogs, rats, hamsters, mice, and from human hearts. *Circ Res*. 1985;56:377-391.
21. Kim JW, Tchernyshyov I, Semenza GL, Dang CV. HIF-1-mediated expression of pyruvate dehydrogenase kinase: a metabolic switch required for cellular adaptation to hypoxia. *Cell Metab*. 2006;3:177-185.
22. Papandreou I, Cairns RA, Fontana L, Lim AL, Denko NC. HIF-1 mediates adaptation to hypoxia by actively downregulating mitochondrial oxygen consumption. *Cell Metab*. 2006;3:187-197.
23. Semenza GL. Hypoxia-inducible factors in physiology and medicine. *Cell*. 2012;148:399-408.
24. Huttemann M, Lee I, Pecinova A, Pecina P, Przyklenk K, Doan JW. Regulation of oxidative phosphorylation, the mitochondrial membrane potential, and their role in human disease. *J Bioenerg Biomembr*. 2008;40:445-456.
25. Murry CE, Jennings RB, Reimer KA. Preconditioning with ischemia: a delay of lethal cell injury in ischemic myocardium. *Circulation*. 1986;74:1124-1136.

26. Kobara M, Tatsumi T, Matoba S, et al. Effect of ischemic preconditioning on mitochondrial oxidative phosphorylation and high energy phosphates in rat hearts. *J Mol Cell Cardiol*. 1996;28:417-428.
27. Heckmann BL, Zhang X, Xie X, Liu J. The G0/G1 switch gene 2 (G0S2): regulating metabolism and beyond. *Biochim Biophys Acta*. 2013;1831:276-281.
28. Heckmann BL, Zhang X, Xie X, et al. Defective adipose lipolysis and altered global energy metabolism in mice with adipose overexpression of the lipolytic inhibitor G0/G1 switch gene 2 (G0S2). *J Biol Chem*. 2014;289:1905-1916.
29. Heier C, Radner FP, Moustafa T, et al. G0/G1 switch gene 2 regulates cardiac lipolysis. *J Biol Chem*. 2015;290:26141-26150.
30. Heckmann BL, Zhang X, Saarinen AM, et al. Liver X receptor alpha mediates hepatic triglyceride accumulation through upregulation of G0/G1 Switch Gene 2 expression. *JCI Insight*. 2017;2:e88735.
31. Barbour RL, Sotak CH, Levy GC, Chan SH. Use of gated perfusion to study early effects of anoxia on cardiac energy metabolism: a new 31P NMR method. *Biochemistry*. 1984;23:6053-6062.
32. Yoshida T, Alfaqaan S, Sasaoka N, Imamura H. Application of FRET-based biosensor "ATeam" for visualization of ATP levels in the mitochondrial matrix of living mammalian cells. *Methods Mol Biol*. 2017;1567:231-243.
33. Nagao T, Shintani Y, Hayashi T, et al. Higd1a improves respiratory function in the models of mitochondrial disorder. *FASEB J*. 2019:1-13. https://doi.org/10.1096/fj.201800389R

SUPPORTING INFORMATION

Additional supporting information may be found online in the Supporting Information section.

How to cite this article: Kioka H, Kato H, Fujita T, et al. In vivo real-time ATP imaging in zebrafish hearts reveals G0s2 induces ischemic tolerance. *The FASEB Journal*. 2020;00:1–14. https://doi.org/10.1096/fj.201901686R